Available online at www.sciencedirect.com
ScienceDirect
Journal of the European Ceramic Society 29 (2009) 1665–1677
www.elsevier.com/locate/jeurceramsoc

In vitro characterisation of plasma-sprayed apatite/wollastonite glass–ceramic biocoatings on titanium alloys

V. Cannillo [a,*], J. Colmenares-Angulo [b], L. Lusvarghi [a], F. Pierli [a], S. Sampath [b]

[a] *Dipartimento di Ingegneria dei Materiali e dell'Ambiente, Università di Modena e Reggio Emilia, Via Vignolese 905, 41100 Modena, Italy*
[b] *Center for Thermal Spray Research, State University of New York, Stony Brook, NY 11784-2275, USA*

Received 1 August 2008; received in revised form 10 September 2008; accepted 20 September 2008
Available online 5 November 2008

Abstract

Some ceramics have the ability to form direct bonds with surrounding tissues when implanted in the body. Among bioactive ceramics, the apatite/wollastonite (A/W) glass–ceramic, containing apatite and wollastonite crystals in the glassy matrix, has been largely studied because of good bioactivity and used in some fields of medicine, especially in orthopaedics and dentistry. However, medical applications of bioceramics are limited to non-load bearing applications because of their poor mechanical properties. In this study, A/W powders, obtained from industrial and high grade quality raw materials, were thermally sprayed by APS (atmospheric plasma spraying) on Ti–6Al–4V substrates, in order to combine the good bioactivity of the bioceramic and the good mechanical strength of the titanium alloy base material. The microstructure and the resulting properties were evaluated depending on processing parameters and post-processing thermal treatments. The morphology and the microstructure of the coatings were observed by SEM and the phase composition was examined by X-ray diffraction. The bioactivity of the coatings was evaluated by soaking the samples in a simulated body fluid (SBF) for 1, 2 and 5 weeks. The bioactive behaviour was then correlated with the thermal treatments and the presence of impurities (in particular Al_2O_3) in the coatings.

Keywords: Apatite; Wollastonite; Biocoatings; Glass–ceramics; Plasma spraying

1. Introduction

Some composition of glasses, ceramics and glass–ceramics have been shown to bond to bone tissues.[1–5] These materials are known as bioactive ceramics: the surface is able to form a biologically active hydroxycarbonate apatite (HCA) layer which provides the bonding interface with biological tissues. The HCA phase that forms on bioactive implants is similar to the mineral phase in bone, both chemically and structurally.[6,7] In the 1980s, Kokubo et al. developed a bioactive material, containing apatite and wollastonite crystals in the glassy matrix, labelled apatite/wollastonite (A/W) glass–ceramic, in the $MgO–CaO–SiO_2–P_2O_5$ system.[8–17] A/W glass–ceramic can form a tight chemical bond with bone and can produce a high mechanical strength, compared to other ceramics.[8–12,18,19] It is currently used in medical applications, either in powder form as bone filler or as a bulk material.[9] However, the A/W glass–ceramic, due to its relatively low fracture toughness, cannot be used in load bearing applications, such as in femoral and tibial bones. In these applications, metallic materials such as stainless steel, Co–Cr–Mo alloys and titanium alloys are used.[20] However, these materials do not directly bond to living bone. The problem can potentially be solved by applying bioceramic coatings onto metal substrates. For this reason, different coating techniques have been introduced such as dip coating, electrophoretic deposition, sintering, hot isostatic pressing, flame spraying and plasma spraying.[21,22] One of the most accepted and commercialised bioactive coating is the plasma-sprayed hydroxyapatite (HA) coating.[23–28] The advantages of the plasma-spray technique are the high deposition rate and the high bonding rate between the plasma-sprayed biocoatings and human tissues. The HA-coated implants still have some serious drawbacks resulting in significant challenges in their expanded utilisation.[29] Moreover, there were some attempts to deposit bioactive glass coatings, also in combination with HA,[22,29–36] but to the best of the authors' knowledge, the A/W glass ceramic has not been deposited by plasma spraying up to date.

* Corresponding author. Tel.: +39 059 2056240; fax: +39 059 2056243.
E-mail address: valeria@unimore.it (V. Cannillo).

0955-2219/$ – see front matter © 2008 Elsevier Ltd. All rights reserved.
doi:10.1016/j.jeurceramsoc.2008.09.022

Following the industrial success of plasma-sprayed HA as a bioceramic coating and, in an attempt to widen the use of A/W glass–ceramic, taking advantage of the high stiffness and bioactivity, in this work powders with A/W composition have been plasma sprayed onto a titanium alloy. Since it has been reported that the crystals of wollastonite can enhance the mechanical strength and the crystals of apatite can promote the bioactivity of this glass–ceramic,[9,37] the as-sprayed A/W was thermally treated in order to have apatite and wollastonite crystals in the glassy matrix. It has been demonstrated that if the A/W glass–ceramic, which forms apatite and wollastonite crystals during devetrification, contains also Al_2O_3 in the glassy matrix, it does not bond to living bone and does not form an apatite layer on the surface both in SBF and in vivo.[13] Ohtsuki et al.[16] found that the addition of 1.7 mol% Al_2O_3 to the Kokubo composition of the A/W glass–ceramic was enough to inhibit its bioactivity.

In the present research, two different A/W frits were used as starting feedstock for thermal spraying. The frits, labelled AWC and AWP, differed for the raw materials used in the preparation and for the granulometry. Economic reasons led to the utilisation of industrial raw materials for the AWC frit. Moreover, the AWC frits used were coarse, in order to have a better flowability in the thermal spray equipment. High purity raw materials were used for the AWP frits, in order to accurately control the chemical composition and thus to have less impurities in the thermally sprayed coatings. Moreover, in order to enhance the microstructure, the AWP frits were chosen finer in comparison with the AWC frits, even if some problems associated with the flowability arose.

It is worth noting that this study is the first attempt to thermally spray the A/W glass–ceramics onto a titanium alloy for potential biomedical applications, thus coupling the toughness of the substrate with the bioactivity of the coating. The aim of the present work was to determine the bioactivity behaviour of the as-sprayed and thermally treated AWC and AWP coatings, correlated with the presence of Al_2O_3 in the composition, the morphology and the crystalline phases formed. This could be a valuable alternative to commercial HAp-coated titanium implants, since, as mentioned, the A/W glass–ceramic is more bioactive (i.e., higher bioactivity index) than commercial HA and has better mechanical properties.[3] The bioactivity of the coatings was analysed by immersion in a TRIS-buffered simulated body fluid (SBF) with an ion concentration nearly equal to that of human blood plasma, as proposed by Kokubo et al.[15] for the in vitro study of the A/W glass–ceramic. The changes in calcium, phosphate, magnesium and silicon ion concentration after soaking in SBF were evaluated by ICP-AES. X-ray diffractometer (XRD) analysis was used to identify the crystalline phases. Scanning electron microscopy (SEM) was used to observe the morphology and the characteristics of the coatings, both in surface and in cross-sections. Energy dispersive X-rays spectroscopy (EDS) was employed to analyse the chemical composition.

2. Materials and methods

The glass composition reported by Kokubo et al.[8–14] is shown in Table 1. Two different frits were employed in this investigation: AWC and AWP, with the same nominal composition but obtained with different raw materials. The batch mixtures for AWC were prepared from industrial raw materials of: SiO_2, $MgCO_3$, $CaCO_3$, $Ca_3(PO_4)_2$ and CaF_2. The batch mixtures for AWP were prepared from commercial pure raw material of: SiO_2 (Carlo Erba, Italy), $MgCO_3$ (Acros, Italy), $CaCO_3$ (Carlo Erba, Italy), $Ca_3(PO_4)_2$ (Carlo Erba, Italy) and CaF_2 (Carlo Erba, Italy). The batches were placed in a platinum crucible and melted in an electric furnace at 1550 °C for 1 h.

Glass powders were obtained by fritting the glass in water. The AWC and AWP frits were milled with a fast planetary moving mill, with Al_2O_3 balls and in dry conditions. The size of the powders was controlled by sieving: AWC were in the 75–125 μm range, AWP in the 45–75 μm range.

The AWC and AWP powders were plasma-sprayed on Ti–6Al–4V substrates using a system equipped with a F4MB torch, in APS mode, using the operating parameters listed in Table 2.

The powders were subjected to chemical analysis (ICP-AES, Varian, Liberty 200), in order to evaluate the real chemical composition of the frit. The powders were characterised by means of DTA analysis (Netzsch DSC 404 Differential Thermal Analyzer), using 30 mg of powders heated from 20 °C to 1400 °C at 10 K/min, in order to obtain the critical temperatures of the frits, such as glass transition and crystallisation temperatures. Density measurements were performed through a He picnometry (AccuPyc 1330, Micromeritics). Sintering tests on pressed powders were carried out with a hot stage microscope (Misura HSM ODHT, Expert System Solutions, Italy) to find the sintering temperature of the frit. Bulk AWC and AWP glass samples were obtained by pouring the glass into a carbon made container and then annealed at 760 °C for 1 h, in order to obtain 15 mm × 5 mm × 5 mm bars (from bulk samples by cutting and grinding), useful for dilatometry tests (DIL 404, Netzsch).

The substrates of Ti–6Al–4V, having dimensions of 25 mm × 2 mm × 180 mm, were pre-grit blasted with alumina particles before deposition.

In order to improve the microstructure and the mechanical properties of the as-sprayed AWC coatings by sintering and crystallization, thermal treatments were performed in an

Table 1
Nominal and real composition in oxides (wt%).

Composition wt%	SiO_2	P_2O_5	CaO	CaF_2	Al_2O_3	MgO	Others
Nominal composition[9]	34	16.2	44.7	0.5	–	4.6	–
Real composition of AWC	33.30	13.30	48.20	0.03	1.90	1.92	1.35
Real composition of AWP	33.20	15.50	46.20	0.06	0.20	4.30	0.54

Table 2
Plasma torch operating parameters.

Operating parameters	Ar flow [slpm]	H_2 flow [slpm]	Current [A]	Voltage [V]	Feed rate [rpm]	Nozzle diameter [mm]	Spraying distance [mm]
AWC	47.4	8.5	550	64.9	15	8	70
AWP	42	9	600	66	20	8	70

electric furnace. The heating rate was 10 K/min in all cases. On the basis of the glass transition and crystallisation temperatures from DTA analysis, different crystallisation isotherms were chosen, in order to obtain sintered and crystallised coatings, with a good microstructure. Crystallization isotherms at 800 °C, 825 °C, 850 °C, 900 °C and 950 °C for 1 h were performed only on AWC coatings, for economical reasons, in order to have a screening of the crystallisation phenomena. Since it has been found that the best coating microstructure was obtained with a thermal treatment at about 900 °C for 1 h, crystallization isotherm at 900 °C for 1 h was performed also on AWP coatings. All the samples were cooled to room temperature inside the furnace after heat treatments.

The as-sprayed and the thermally treated coatings characterisation was performed with scanning electron microscopy (ESEM Quanta-200, coupled with EDS Oxford INCA 350)—both in surface and in cross-sections (mounted in resin, ground with 800 mesh, 1000 mesh and 2000 mesh SiC papers and polished with 3 μm and 0.5 μm poly-crystalline diamond suspension). X-ray diffraction analysis (X'PERT PRO), from 15° to 70° 2θ at a speed of 2°/min with 0.02° increment, using Cu-Kα at 40 kV and 40 mA, was performed on the coatings surfaces.

The in vitro study was carried out on the as-sprayed AWC and the as-sprayed AWP. The thermally treated AWC and AWP at 900 °C for 1 h were also characterised with in vitro tests in SBF. To evaluate the effect of the temperature of the thermal treatments, the AWC coatings thermally treated at 800 °C were immersed in SBF, too. According to the procedure described by Kokubo et al.[15] all the samples of dimensions of 5 mm × 4 mm × 2 mm were soaked in SBF. The sample were soaked in 50 ml of solution, containing 2 ml of SBF and 48 ml of bidistilled water, for specific interval time: 1, 2 and 5 weeks and placed in a water bath with a constant temperature of 37 °C. The immersion tests were carried out in duplicate. According to the Kokubo procedure the samples were placed in a vertical displacement. The pH measurements were taken at around 37 °C, after each soaking interval, by means of a pH meter (Crison, MicropH). The pH measurements of the solutions were correlated to ion dissolution into the SBF. Changes in the concentration of Si, Ca, Mg and P were measured by inductively coupled plasma atomic emission spectroscopy (ICP-AES) after the removal of the samples from soaking solutions. Both the surface, in low vacuum configuration, and the cross-section, in high vacuum configuration, of the specimens were characterised by environmental scanning electron microscopy (ESEM) coupled with energy dispersive spectroscopy (EDS) before and after each soaking in SBF; X-ray diffraction analysis was performed on the coatings surfaces after each soaking in SBF. The phases formed on the surface were identified by means of an X-ray diffractometer: scans were run from 15° to 70° 2θ at a speed of 2°/min with 0.02° increment, using Cu-Kα at 40 kV and 40 mA.

3. Results and discussion

3.1. Powders and bulk glasses characterisation

The frit chemical analysis is reported in Table 1 as well. For AWC, the real composition was a bit different from the nominal one: in fact the presence of Al_2O_3 in the amount of 1.9 wt%, corresponding to 1.86 mol%, was mainly due to the raw materials used. The MgO and P_2O_5 weight percentage were lower than that of the nominal composition; moreover in the real composition Fe_2O_3 and Na_2O were present in a very little amount. For AWP, the composition confirmed the nominal one, even if Al_2O_3 was present in a very little amount of about 0.20 wt%, corresponding to about 0.19 mol%. The limited amount of alumina in the AWP frits confirms that no contamination from Al_2O_3 balls took place.

The powders were sieved in order to have an average diameter of the AWC powders superior to 75 μm and an average diameter of the AWP powders inferior to 75 μm.

The AWC glass powders had a density of 2.92 g/cm^3 and the AWP glass powders had a density of 2.94 g/cm^3.

Differential thermal analysis, reported in Fig. 1, indicated that the AWP glass has a T_g at around 754 °C. The DTA curve showed one exothermal crystallization peak (T_p), at around 904 °C. The DTA of the AWC glass was similar to that of AWP glass, with similar critical temperatures. The sintering temperature was about 850 °C and the softening temperature was about 1140 °C, from the hot stage microscope measurements. The softening temperature of AW glass occurred at a high temperature and the collapse of the glass was immediate in the range of 150 °C.

The linear thermal expansion coefficient (50 °C < T < 400 °C) of the AWC glass was 10.08×10^{-6} K^{-1}, whereas for AWP glass was 11.27×10^{-6} K^{-1} (50 °C < T < 400 °C). The linear thermal expansion coefficient (50 °C < T < 400 °C) of the Ti–6Al–4V alloy was 8.7×10^{-6} K^{-1} (50 °C < T < 500 °C).[29]

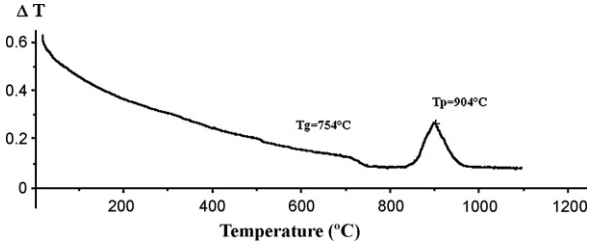

Fig. 1. Differential thermal analysis of AWP glass (heating rate 10 °C/min).

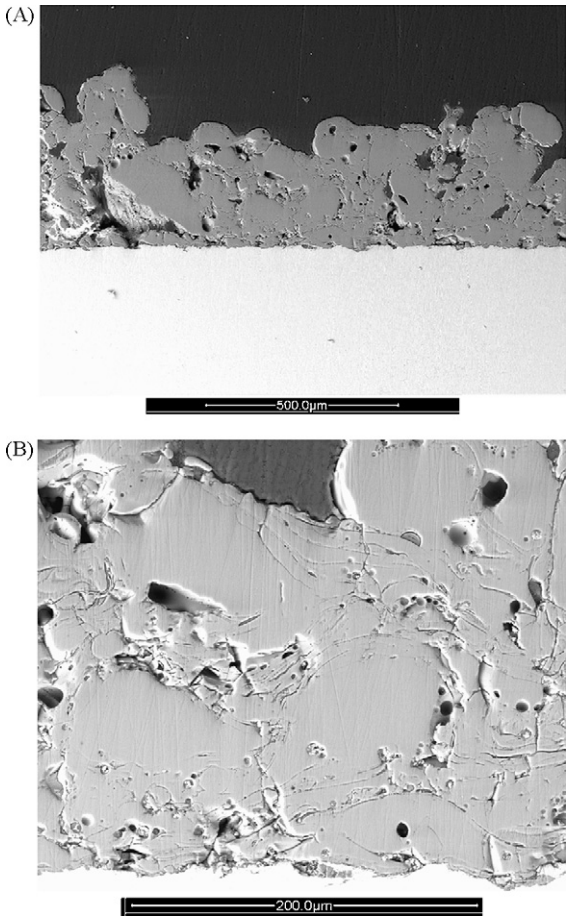

Fig. 2. SEM cross-section of as-sprayed AWC: (A) general view and (B) detail.

3.2. Coatings characterisation

The as-sprayed AWC coating had an average thickness of 240 μm (Fig. 2). The as-sprayed AWC coating presented a highly defective microstructure with unmelted or partially melted particles, globular pores and cracks, even if the adhesion between coating and substrate did not show substantial flaws. The defected microstructure was not only related to the characteristic features of the plasma spray process but also due to non-optimal powder feedstock of these novel non-commercial powders. Nevertheless, the coatings allowed for critical assessment of the bioactive performance. During the thermal treatments sintering occurred, since the pores were rounded, the boundaries intersplats disappeared and a lot of cracks were closed, but the crystallisation process overlapped the sintering strongly limiting the benefit (Fig. 3). The surface roughness of the as-sprayed AWC coating was high because of both the coarseness of the starting powders of the feedstock and the bad flattening of the coarse glass droplets, phenomena already reported in previous works.[e.g. 38] The surface roughness was not changed after the thermal treatments: this was probably due both to the viscosity of the glass that was not low enough at the treatment temperatures and the above mentioned overlapping of the sintering and the crystallisation phenomena. The interfaces between thermally treated coatings and substrates were quite good, except for the thermally treated AWC at 950 °C for 1 h, due to a TiO_2 interlayer formed; the oxidation of the substrate was due to the porosity and to cracks of the glass coatings which allowed oxygen to reach the substrate before closing. This caused a significant cracking at the interface (Fig. 4). Crystallisation took place all along the coating thickness during thermal treatments: there were areas much more crystallised than other ones. The XRD results are reported in Table 3. The as-sprayed AWC coating was glassy, as expected: in fact previous studies about plasma-sprayed glass coatings demonstrated this phenomena.[e.g. 39] After the thermal treatment at 800 °C for 1 h, traces of oxyapatite crystals (JCPDS 89-6495), labelled as OHA, could be detected (Table 3), even if the crystals could not be clearly observed in SEM cross-sections (Fig. 3A). After the thermal treatment at 825 °C on AWC coating, diopside crystals (JCPDS 17-0318), labelled as D, started to appear. The thermally treated AWC coating at 850 °C for 1 h (Fig. 3B) was quite similar to that treated at 825 °C, since OHA and D crystals were both detected. The wollastonite crystals (JCPDS 42-0550), labelled as W, appeared after the thermal treatment at 900 °C (Fig. 3C) and the peaks of D decreased. After the thermal treatment at 950 °C (Fig. 3D) the peaks of W increased and the peaks of D decreased, as reported in Table 3.

The AWC thermally treated at 900 °C for 1 h was the best compromise to have an apatite/wollastonite glass–ceramic with a good microstructure.

The AWC as-sprayed and thermally treated at 900 °C for 1 h were therefore characterised after the in vitro test to compare the bioactivity of the coatings in SBF (Tables 4 and 5, as described in details in the following paragraph). Moreover, a thermally treated AWC coating at 800 °C for 1 h was soaked in SBF, to compare the bioactivity in relation with the different temperatures of the thermal treatments.

The as-sprayed AWP coating had an average thickness of about 110 μm and presented a defective microstructure with a weak interface with the substrate and a lot of pores (Fig. 5). The as-sprayed AWP coating was partially crystallised with crystals of oxyapatite, labelled OHA, (JCPDS 89-6495) and wollastonite, labelled W, (JCPDS 42-0550), as reported in Table 6. This result was unexpected because almost all the former studies on thermally sprayed glasses related a complete absence of crystalline phases in the as-sprayed conditions, with the only reported peaks belonging to unprocessed (unmelted) raw materials from the glass powder manufacturing[38,39] or to a specific set of spraying parameters in a DOE.[40] The investigation of this outcome is not the aim of this present study, but further measurements will be carried out to better understand the presence of devetrification in the as-sprayed AWP sample.

The AWP coatings thermally treated at 900 °C for 1 h did not show a detectable change in roughness in comparison with the as-sprayed AWP (Fig. 6). The XRD spectrum (Table 7) showed the presence of OHA (JCPDS 89-6495), W (JCPDS 42-0550) crystals in the thermally treated AWP. The interface was affected by a TiO_2 layer, due to the reaction between oxygen and the Ti of the substrate, but delamination did not occur.

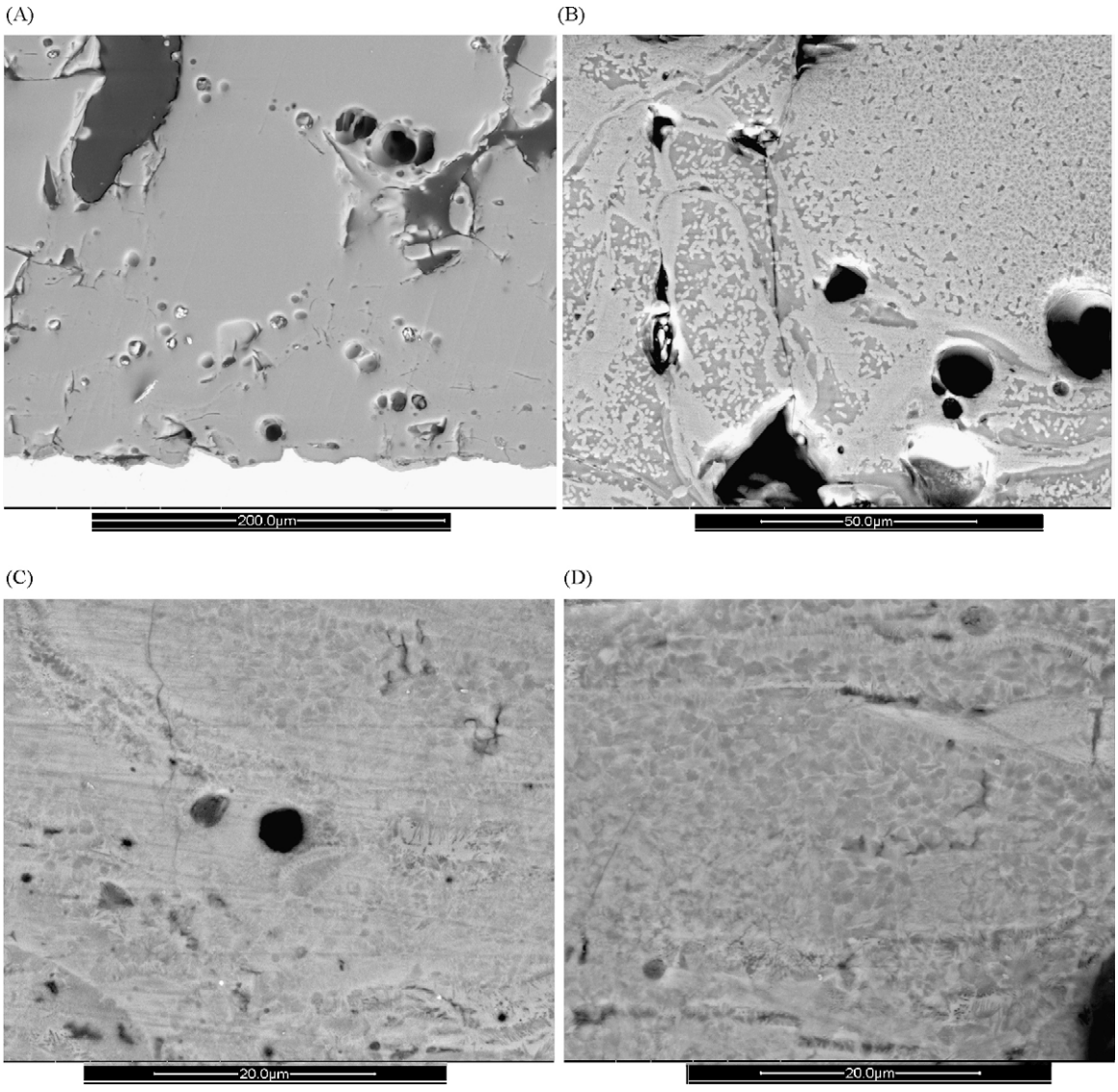

Fig. 3. SEM cross-sections of thermally treated AWC: (A) at 800 °C, (B) at 850 °C, (C) at 900 °C and (D) at 950 °C.

Table 3
Crystalline phases found in the AWC coatings as-sprayed and after different thermal treatments at: 800 °C, 825 °C, 850 °C, 900 °C and 950 °C for 1 h.

Sample	Glassy phase	Oxyapatite (JCPDS 89-6495)	Diopside (JCPDS 17-0318)	Wollastonite (JCPDS 42-0550)
AWC as sprayed	+++	None	None	None
AWC 800 °C 1 h	++	+	None	None
AWC 825 °C 1 h	+	++	++	None
AWC 850 °C 1 h	None	++	+	Traces
AWC 900 °C 1 h	None	+++	Traces	++
AWC 950 °C 1 h	None	+++	Traces	+++

Table 4
Crystalline phases found in the AWC coatings as-sprayed before and after soaking in SBF for 1, 2 and 5 weeks.

AWC as-sprayed in SBF	Glassy phase	Hydroxyapatite (JCPDS 73-1731)
0 week	+++	None
1 week	++	+
2 weeks	++	++
5 weeks	+	++

The AWP as-sprayed and thermally treated at 900 °C for 1 h were characterised after the in vitro test to compare the bioactivity of the coatings in SBF, as described in details in the following paragraph.

3.3. In vitro tests and characterisation

After the soaking of as-sprayed AWC coatings in SBF for 1 week, a thin layer of a bone-like apatite was observed by

Table 5
Crystalline phases found in the thermally treated AWC coatings at 900 °C for 1 h, before and after soaking in SBF for 1, 2 and 5 weeks.

AWC thermally treated at 900 °C after soaking in SBF	Glassy phase	Oxyapatite (JCPDS 89-6495)	Wollastonite (JCPDS 42-0550)
0 week	None	+++	++
1 week	None	+++	++
2 weeks	None	+++	++
5 weeks	None	+++	++

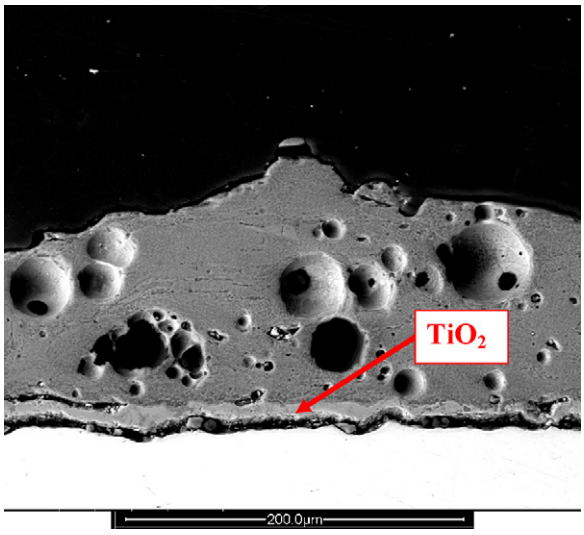

Fig. 4. SEM cross-sections of thermally treated AWC at 950 °C; a TiO_2 layer at the substrate-coating interface caused by the surface oxidation of the titanium alloy is clearly visible above the cracks running along the interface.

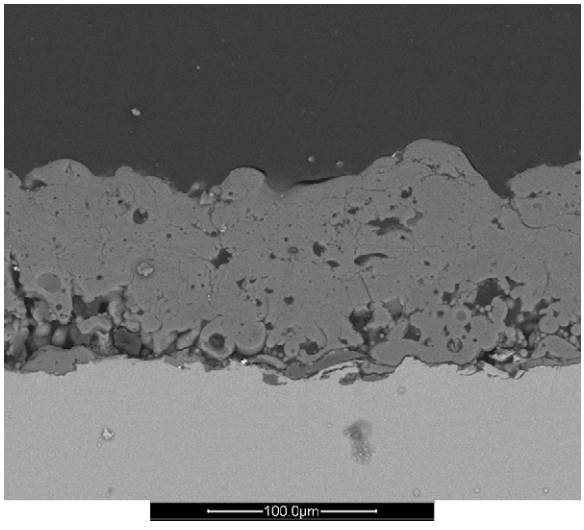

Fig. 5. SEM cross-section of as-sprayed AWP.

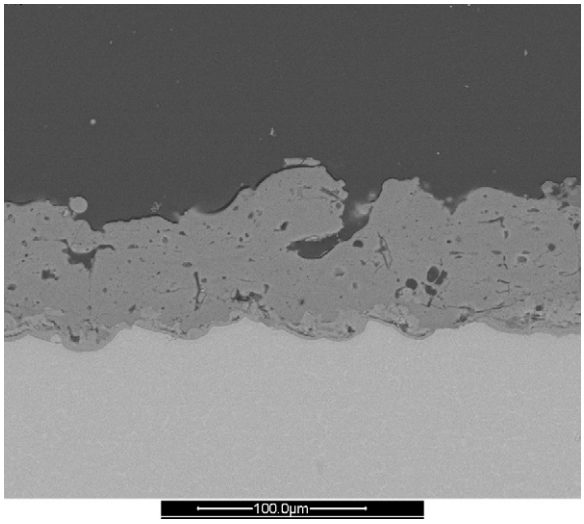

Fig. 6. SEM cross-section of thermally treated AWP at 900 °C for 1 h.

SEM on the surface (Fig. 7A) and inside the pores of the coating connected to the surface (Fig. 7B). A small SiO_2-rich layer was present under the apatite layer, which increased in thickness as a function of time of soaking (Fig. 7C). The Ca/P ratio of the bone-like apatite layer was about 1.62 after 5 weeks of soaking, as calculated from EDS spectrum (semi-quantitative analysis in Fig. 8). The Ca/P ratio of a crystalline hydroxyapatite should be about 1.67, from ISO 13779-3 standard, which is close to the Ca/P ratio found for the bone-like apatite layer of the present study. The bone-like apatite layer after 5 weeks of soaking in SBF was crystallised and the crystalline HCA layer formed was nearly equivalent to biological apatite grown in vivo. Fig. 7A illustrates that the interface between the underlying coating and bone-like apatite layer was poor due to extensive cracking all along it; besides, cracks perpendicular to the interface were also present. Moreover, the preparation of the samples for the SEM observations, i.e., mechanical polishing, may have increased the cracks of the already damaged and quite brittle apatite layer. The thickness of bone-like apatite layer was quite constant with the time of soaking while the thickness of

Table 6
Crystalline phases found in the as-sprayed AWP coatings before and after the immersion in SBF 1, 2 and 5 weeks.

AWP as-sprayed, after soaking in SBF	Glassy phase	Oxyapatite (JCPDS 89-6495)/hydroxyapatite (JCPDS 73-1731)	Wollastonite (JCPDS 42-0550)
0 week	+	+	+++
1 week	+	+	++
2 weeks	+	++	++
5 weeks	+	++	+

Table 7
Crystalline phases found in the thermally treated AWP coatings at 900 °C for 1 h, before and after soaking in SBF for 1, 2 and 5 weeks.

AWP thermally treated at 900 °C, after soaking in SBF	Glassy phase	Oxyapatite (JCPDS 89-6495)/ hydroxyapatite (JCPDS 73-1731)	Wollastonite (JCPDS 42-0550)
0 week	None	++	+++
1 week	None	++	++
2 weeks	None	++	++
5 weeks	None	+++	+

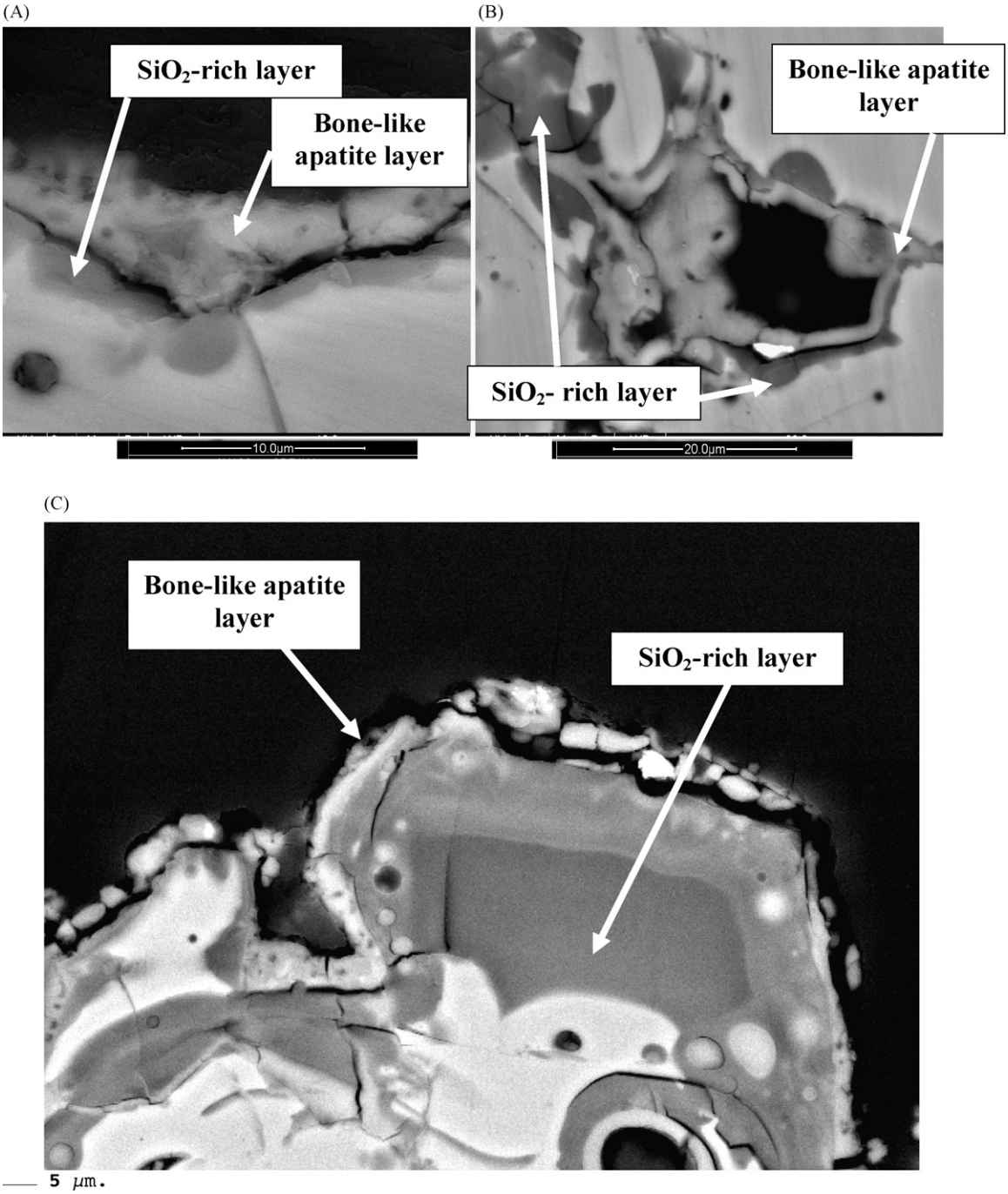

Fig. 7. SEM cross-sections of AWC as-sprayed coating after soaking in SBF: (A) 1 week: surface, (B) 1 week: surface connected pore and (C) 5 weeks.

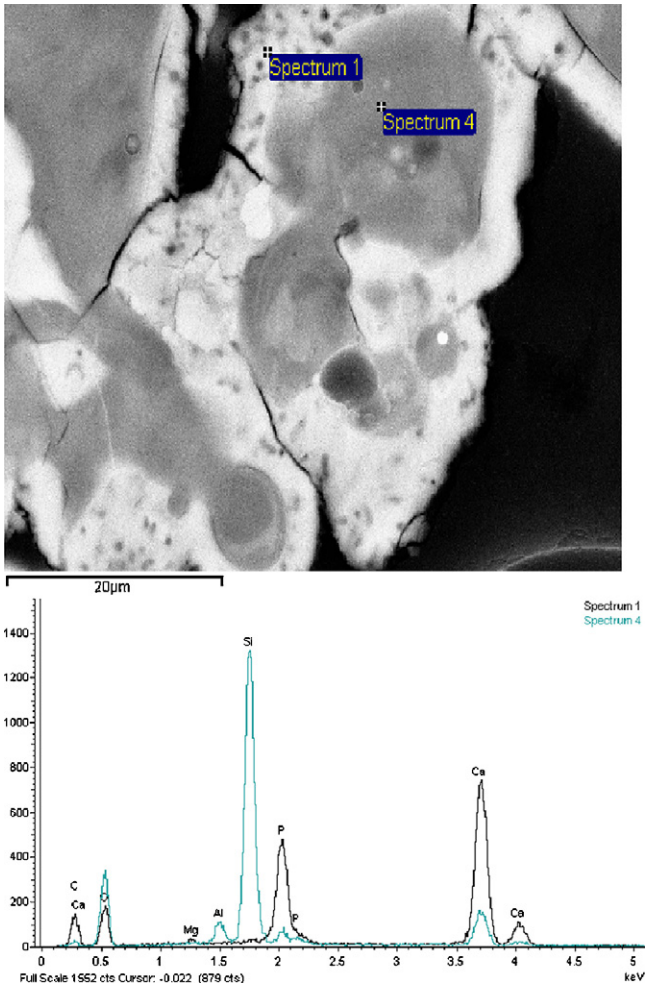

Fig. 8. SEM cross-section and EDS spectrum of AWC as-sprayed after soaking 5 weeks in SBF (spectrum 1: bone-like apatite layer, spectrum 4: SiO_2-rich layer).

SiO_2-rich layer increased, as shown in the graph in Fig. 9. In the literature a similar behaviour is reported.[4,5] Peitl et al.[41] studied the characteristic double layer formation on the surface of a bioactive P_2O_5–Na_2O–CaO–SiO_2 glass, including the network dissolution of the glass, the silica-gel layer formation, the

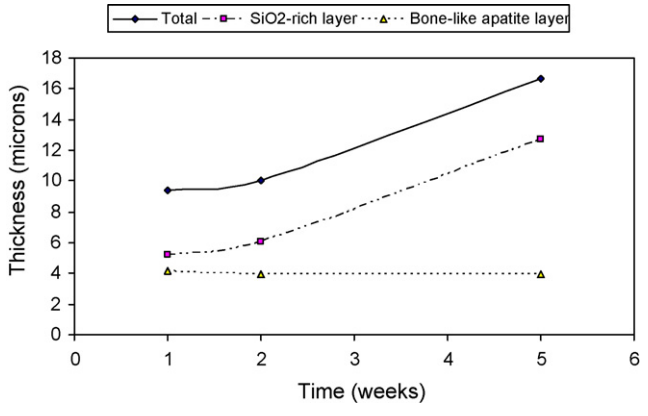

Fig. 9. Thickness of the bone-like apatite layer + SiO_2-rich layer on AWC coatings versus time of soaking in SBF.

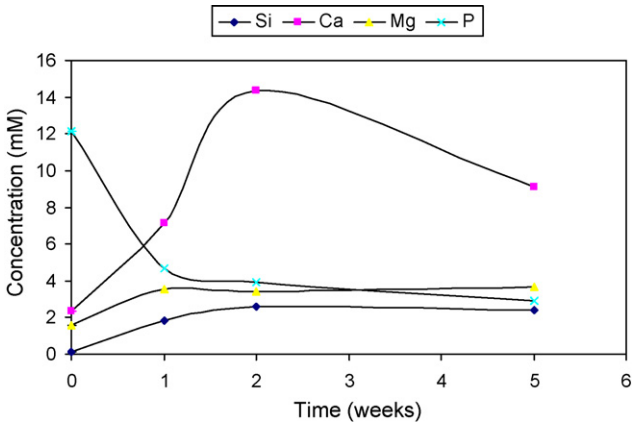

Fig. 10. Ion release of Si, Ca, Mg and P (mM) vs. time of solutions of AWC as-sprayed soaked in SBF.

amorphous calcium phosphate precipitation and the HCA crystallisation. Since the amorphous phase was predominant in the A/W coating, the bioactivity mechanism was similar to that of bioactive glasses.

Table 4 reports the XRD results of AWC as-sprayed before and after the immersion in SBF. The as-sprayed AWC coating was amorphous and after the first week of immersion in SBF the hydroxyapatite (JCPDS 073-1731), labelled HA, was the main phase detected on the surface of the sample. After the second and the fifth week in SBF, the sample became less amorphous, with an high level of HA crystals, corresponding to a formation of a more crystallised bone-like apatite. Fig. 10 shows the changes in calcium, phosphate, magnesium and silicon ion concentration in SBF with immersion time of AWC as-sprayed coatings. The level of magnesium ion concentration in SBF increased a little in time, even if it remained quite constant at about 3 mM after the first week of immersion. Also the silicon ion concentration increased in time until the second week of soaking and then remained constant at about 2.5 mM. A marked decrease in the phosphorous ion concentration was observed in time, while the calcium ion concentration first increased until the second week of soaking and then decreased with time. The AWC as-sprayed coatings released large amounts of calcium ions into the SBF immediately after the immersion in SBF, reaching 14 mM of concentration. From previous works,[17,42] the release of calcium ions from glass–ceramic A/W is expected, since on immersion the calcium ions increase the degree of supersaturation of the surrounding fluid with respect to apatite. Subsequently, the decrease of calcium and phosphorous is correlated to the formation of the bone-like apatite layer; in fact these ions supplied by the surrounding SBF are necessary for the formation of the apatite layer.

Evidence from the literature suggests that a biologically active layer of hydroxycarbonate apatite (HCA) must be formed on the surface of the implanted material; this is probably the common feature of all bioactive materials known to date. The ability of bioactive glasses to bond to bone tissue is a result of their chemical reactivity in physiological media. The underlying bonding mechanism was first reported by Hench[4] and involves different steps. In the AWC coating the first step of

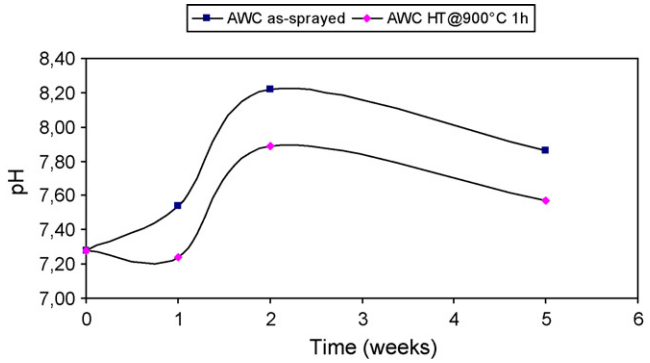

Fig. 11. pH measurements vs. time of solutions of AWC as-sprayed and thermally treated at 900 °C for 1 h after soaking in SBF.

leaching through the exchange of protons from the physiological medium with labile network-modifying ions such as Ca^{2+} and Mg^{2+} went on until the second week of immersion in SBF. The pH increased until 8.2 in the first 2 weeks of soaking, due to the release of alkaline ions in the solution (Fig. 11). This environment facilitated the dissolution of the network and formation of additional silanol groups, as well as the loss of soluble silica as $Si(OH)_4$ that passed into the solution.[5] In fact the silicon ion concentration increased with time (Fig. 10). The silicate ions, with silanol group available for bonding, were released from the glass and attached to a collodion film. These groups were then able to combine with calcium ions to form a calcium silicate. The calcium silicate reacted with the phosphate that was eventually transformed into a crystalline apatite with a higher Ca/P ratio of 1.67—that of a bone-like apatite. The dissolution of calcium might contribute to the formation of apatite, while the dissolution of silicon provides favourable sites for apatite nucleation, according to Kokubo's study on A/W.[14]

After the thermal treatment at 900 °C for 1 h, the amorphous AWC coating became a glass–ceramic coating with oxyapatite and wollastonite crystals in the glassy matrix. The thermally treated AWC at 900 °C showed better mechanical properties with respect to the as-sprayed AWC coating: in fact the Vickers microhardness of the thermally treated coating was higher, with values around 420 $HV_{0.025}$ with respect to 350 $HV_{0.025}$. After the immersion in SBF for 1, 2 and 5 weeks, the thermally treated AWC coatings did not show a bioactive behaviour. In fact even after 5 weeks of immersion in SBF a bone-like apatite layer was not detected on the surface of the samples by SEM (Fig. 12A). The XRD spectrum (Table 5) confirmed that oxyapatite (OHA) and wollastonite (W) crystals were present before and after the soaking in SBF but apatite peaks were due only to the crystallisation induced by the thermal treatment. The absence of a bone-like apatite layer on the surface of the thermally treated AWC coatings at 900 °C was probably due both to the thermal treatment and to the composition of the glass–ceramic. In fact a previous work[43] revealed that the bioactivity of glass–ceramics depends mainly on the amount and the composition of the glassy phase between the crystalline phases formed. Moreover, both Kitsugi et al.[13] and Andersson et al.[44] demonstrated that glass–ceramics containing Al_2O_3 in the glassy matrix are not bioactive. Furthermore thermal treatments on plasma-sprayed bioactive coatings of hydroxyapatite make the coatings not bioactive.[45]

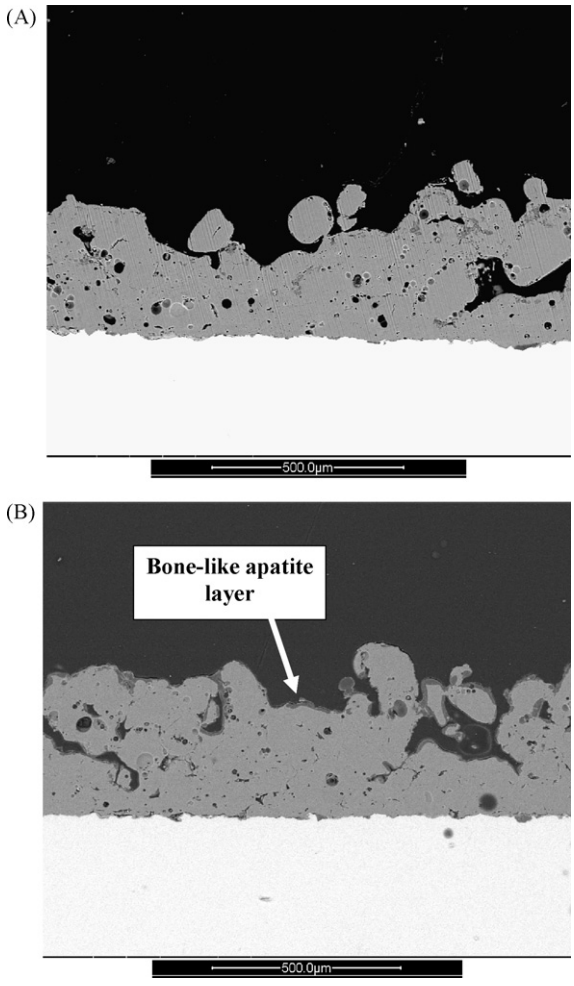

Fig. 12. SEM cross-sections of thermally treated AWC after 1 week of soaking in SBF: (A) thermal treatment at 900 °C for 1 h and (B) thermal treatment at 800 °C for 1 h.

Fig. 13 shows the changes in calcium, phosphorous, magnesium and silicon ion concentration in SBF with immersion time of AWC thermally treated coatings. The level of magnesium ion concentration in SBF was constant at a value of about 2 mM. The silicon ion concentration increased in time until the second

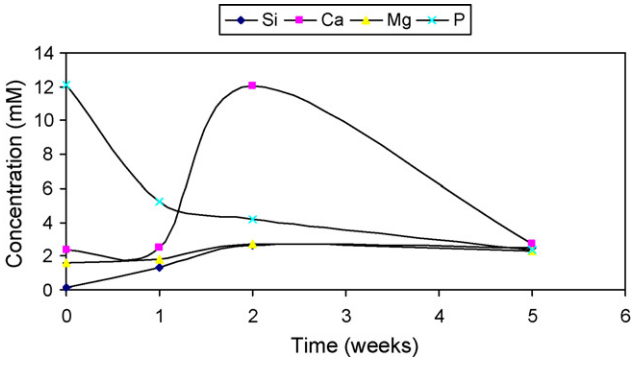

Fig. 13. Ion release of Si, Ca, Mg and P (mM) vs. time of solutions of thermally treated AWC at 900 °C for 1 h after soaking in SBF.

week of soaking after that it stabilised at about 2 mM. The ion concentration of calcium varied with time: initially it decreased a little, then increased until the second week of soaking, reaching 11 mM of concentration and finally, after 5 weeks of soaking, reached about 2 mM of concentration. The ion release of calcium from the thermal treated AWC coating was always less than the release from the as-sprayed one: in fact after 1 week of soaking the calcium ion concentration was 3 mM instead of 7 mM of the as-sprayed AWC coating. During the heat-treatment process, the concentrations of alkali and alkaline ions decreased in the glassy matrix and this led to hinder the ion exchange between the alkali ions from glass–ceramic samples and H^+ or H_3O^+ from SBF solution, which could explain the absent bioactivity of the glass–ceramics thermally treated at 900 °C. The pH behaviour in Fig. 11 confirmed the results from ICP-AES analysis. In fact the pH initially decreased a little, due to the release of network-modifying ions such as Ca^{2+} and then increased until the second week, corresponding to a possible deposition of $CaCO_3$, since the concentration of Si, Mg, and P ions was constant after the second week of soaking. The deposition of $CaCO_3$ crystals was probably removed by the sample water washing after each extraction, and therefore they were not detected by the SEM.

Upon subjecting the amorphous AWC coating to a specific thermal treatment at 800 °C for 1 h, few oxyapatite crystals were present in a predominant glassy matrix. After the thermal treatment at 800 °C only few oxyapatite crystals were present in the coating with a predominant glassy matrix, while after the thermal treatment at 900 °C the coating was mainly crystalline with oxyapatite and wollastonite crystals (Table 3). The behaviour of the AWC coating thermally treated at 800 °C for 1 h was completely different after soaking in SBF from the behaviour of the AWC thermally treated at 900 °C for 1 h: in fact a bone-like apatite layer could be observed on the surface of the coatings after 1 week of soaking from SEM cross-sections (Fig. 12B).

The bioactive mechanism of the as-sprayed and the thermally treated at 800 °C coatings was the same, and similar to that of bioactive glasses, since a bone-like apatite was present on a SiO_2-rich layer. Therefore, the as-sprayed and the thermally treated at 800 °C AWC coatings were bioactive materials, while the thermally treated AWC at 900 °C for 1 h seemed to be not bioactive, at least in the first 5 weeks of soaking.

Therefore, an important result of this work is that the bioactivity of the glass–ceramic A/W coatings depends on the amount and on the composition of the glassy matrix between the crystalline phases formed, in particular on the molar percentage of Al_2O_3. In fact the presence of Al_2O_3 in the AWC powder feedstock real composition was 1.86 mol%, that is higher than the critical value of 1.7 mol%, reported by Ohtsuki et al.[16], which inhibits the bioactivity of the A/W glass–ceramic. Moreover, the thermal treatments decreased the bioactivity of the glassy coatings and, in some cases and after specific heat treatments, such as at 900 °C for the AWC coating, a bioactive glass can be transformed into a inert glass–ceramic. At the same time, the devetrification impoverish the matrix of Si, Ca and P ions, while the concentration of aluminium ions in the matrix increases because they do not take part into the crystallization process.

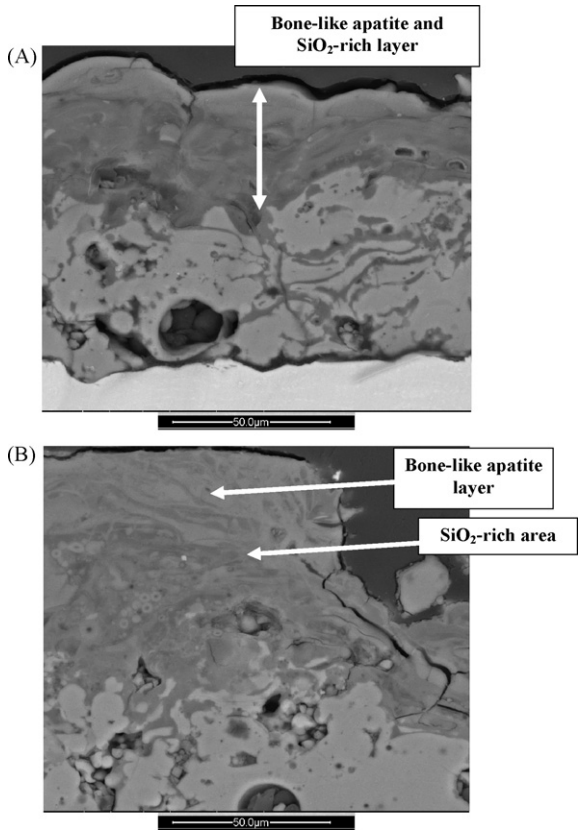

Fig. 14. SEM cross-sections of as-sprayed AWP after soaking in SBF: (A) after 2 weeks and (B) after 5 weeks.

With regard to the in vitro test on the AWP as-sprayed coatings, after 2 weeks of soaking in SBF a bone-like apatite layer was formed on the surface, onto a SiO_2-rich layer (Fig. 14A). The bioactive mechanism, analogous to that of AWC as-sprayed coatings, was the same of bioactive glasses, as reported in the literature.[4,5] Karlsson et al.[46] concluded that for glass to be bioactive, it must form a surface layer of amorphous silica. After the immersion of the as-sprayed AWP in SBF the peaks of apatite increased, while the peaks of wollastonite decreased with time of soaking, coherently with the growth of the bone-like apatite. The bone-like apatite layer increased in time up to 5 weeks (Fig. 14B), even if the apatite layer was mixed with the SiO_2-rich layer through the penetration of the surrounding SBF fluid in the cracks and along the pores.

The pH behaviour (Fig. 15) showed that the pH increased in time first and then decreased. Fig. 16 reports the changes in calcium, phosphate, magnesium and silicon ion concentration in SBF with immersion time for the AWP as-sprayed coating. The level of calcium, silicon and magnesium ion concentration in the SBF immediately increased after the first week of soaking in SBF and a SiO_2-rich layer was formed on the surface of the coating. Hench reported the time-dependent changes of only a single-phase amorphous or glassy material which involve the release of Ca^{2+}, Mg^{2+} ion in the surrounding fluid and the loss of soluble silica to the solution, resulting from the breaking of Si–O–Si bonds and the formation of Si–OH (silanols) at the glassy solution interface.[4] It has been demonstrated that the

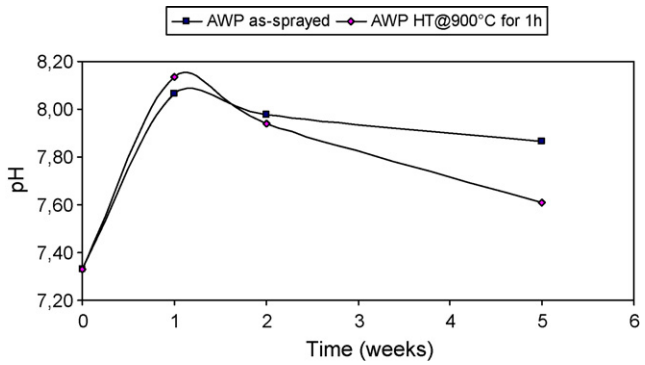

Fig. 15. pH measurements vs. time of solutions of as-sprayed AWP and thermally treated at 900 °C for 1 h after soaking in SBF.

release of silicate ions has a role in the formation of the bone-like apatite layer, since it provides favourable sites for nucleation of apatite on the surface of the coating.[46] After the second week of soaking in SBF a marked decrease in both the calcium and phosphate ion concentration was observed. Simultaneously with this decrease there was the formation of bone-like apatite layer onto the SiO_2-rich layer, since the calcium and phosphate ion, necessary for the formation of the apatite layer, were supplied by the surrounding SBF.

After the immersion in SBF of the thermally treated AWP at 900 °C for 1 h, SiO_2-rich areas were present inside the coating and not only on the surface (Fig. 17A). Only after 5 weeks of soaking a little bone-like apatite layer was visible in SEM cross-section (Fig. 17B). The XRD spectrum (Table 7) confirmed that after 5 weeks of soaking there was an increase in apatite peaks and a decrease in wollastonite peaks. The pH behaviour (Fig. 15 as well) showed that the pH increased in time first and then decreased. Fig. 18 shows the changes in calcium, phosphate, magnesium and silicon ion concentration in SBF with immersion time for the AWP thermally treated coating. The level of calcium, silicon and magnesium ion concentration in the SBF immediately increased after the first week of soaking in SBF. The initial increase in Ca^{2+} concentration might be explained by the dissolution process that released Ca^{2+} into the solution, while the subsequent decrease in Ca^{2+} concentration could be associated with the apatite precipitation process that consumed Ca^{2+} in the solution. The ion release was similar to that of AWP

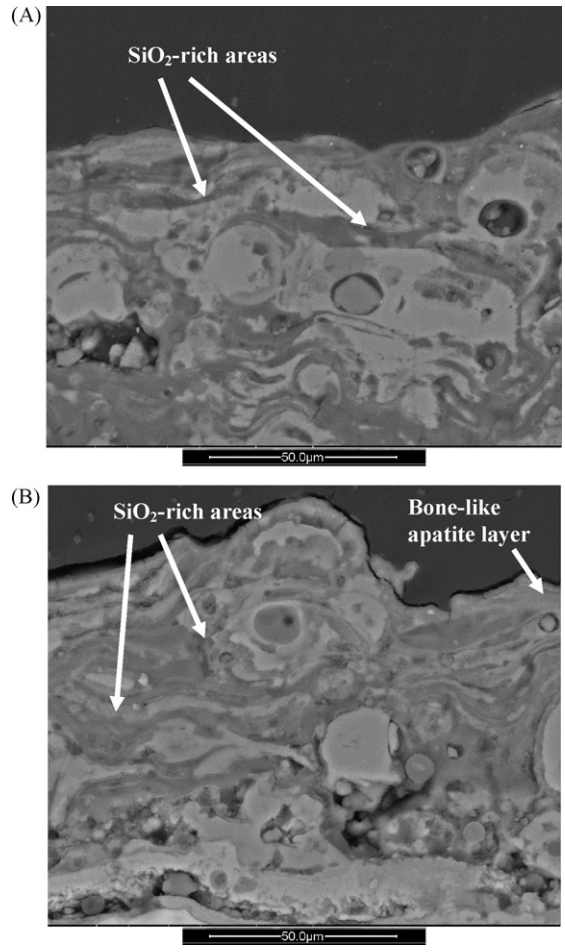

Fig. 17. SEM cross-sections of thermally treated AWP at 900 °C for 1 h after soaking in SBF: (A) after 2 weeks and (B) after 5 weeks.

as-sprayed coating in SBF (Fig. 16), even if the apatite layer could be detected by SEM only after the fifth week.

The glass–ceramic AWP thermally treated at 900 °C was a moderately bioactive coating since after 5 weeks in SBF a little bone-like apatite layer was visible and some SiO_2-rich area were present inside the coatings. The crystallisation in the AWP glassy coatings did not inhibit the bone-like apatite formation during in vitro tests. The bioactive mechanism of the as-sprayed and the thermally treated AWP coatings at 900 °C was simi-

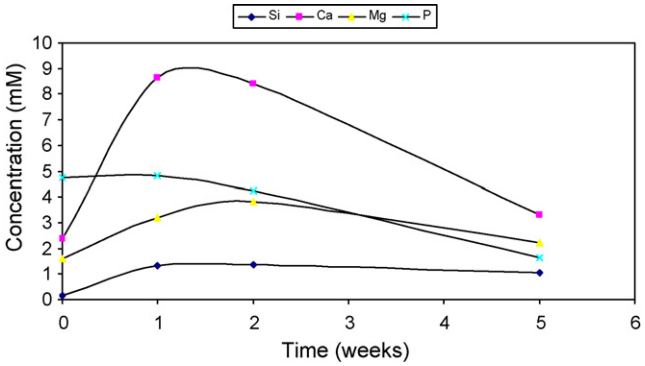

Fig. 16. Ion release of Si, Ca, Mg and P (mM) vs. time of solutions of AWP as-sprayed after soaking in SBF.

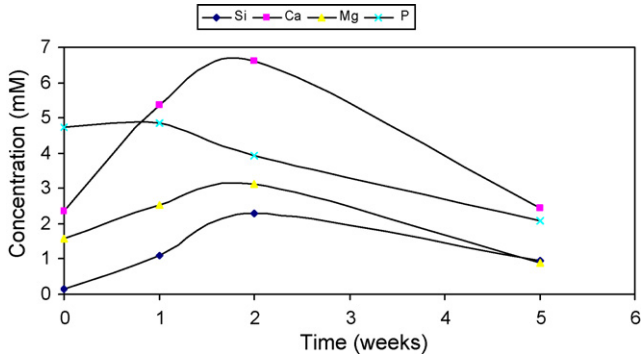

Fig. 18. Ion release of Si, Ca, Mg and P(mM) vs. time of solutions of thermally treated AWP after soaking in SBF.

lar, with a formation of a SiO_2-rich areas inside the coating. The thermal treatments decreased the bioactive behaviour of the plasma-sprayed biocoatings: in fact the as-sprayed AWP coating was more bioactive in comparison with the thermally treated AWP, since in the last one the bone-like apatite layer appeared only after the fifth week in SBF.

The composition and the amount of glassy matrix between the crystalline phases formed mainly influenced the bioactivity of the glass–ceramic AWP coatings, as for AWC coatings. The smaller amount of Al_2O_3 in the glassy matrix ensured the bioactivity of the thermally treated AWP glass–ceramic. In fact the thermally treated AWP coatings, at the same temperature of the AWC coatings at 900 °C for 1 h, showed a bioactive behaviour. This was due to the different amount of Al_2O_3 in the composition: 1.86 mol% for the powder feedstock of AWC coatings and 0.19 mol% for the powder feedstock of AWP coatings. This confirms the Ohtsuki work[16] about the maximum molar percentage of Al_2O_3, of 1.7 mol%, to ensure the bioactivity of the A/W glass–ceramic. Moreover, the presence of Al_2O_3 in the glassy matrix could have played a major role also in the change of the bioactive mechanism: in fact in the AWC coating, with a higher concentration of Al_2O_3 in the composition, the bone-like apatite laid onto a SiO_2-rich layer while in the AWP coating, with a negligible amount of Al_2O_3 in the composition, the bone-like apatite and the SiO_2-rich layers grew together.

4. Conclusions

Bioactivity of plasma-sprayed A/W glass coatings, based on Kokubo A/W composition with different raw materials, industrial (AWC) and high quality (AWP), was investigated.

The as-sprayed and thermally treated coatings were carefully characterised, before and after in vitro tests in SBF for 1, 2 and 5 weeks of soaking.

The as-sprayed AWC and AWP coatings, before thermal treatments, were able to induce the formation of a bone-like apatite onto a SiO_2-rich layer after the soaking in SBF.

The thermal treatments decreased the bioactivity of the coatings and, after specific treatments, some bioactive materials were transformed into inert materials. In particular, the post-heat treatments at 900 °C for 1 h on the as-sprayed AWC and AWP coatings, in order to enhance the microstructure and induce the crystallisation of oxyapatite and wollastonite phases, showed a negative effect on the bioactivity behaviour of the glass–ceramic samples. The thermally treated AWC at 900 °C did not form a bone-like apatite layer on the surface after 5 weeks of soaking in SBF, while the thermally treated AWP was able to form an apatite layer only after 5 weeks in SBF.

The main difference in the bioactivity behaviour of thermally treated AWC and AWP coatings at 900 °C for 1 h could be attributed to the different amount of the Al_2O_3 in the composition. In fact small changes in the amount of Al_2O_3 resulted in significant changes in the bioactivity behaviour of the partially or fully crystallised samples in SBF. As a matter of fact, the thermally treated AWP, with a smaller amount of Al_2O_3 in the glassy matrix, was moderately bioactive while the thermally treated AWC at the same temperature (900 °C for 1 h), with a higher amount of Al_2O_3 in the glassy matrix, was not bioactive at least in the first 5 weeks of soaking.

Upon subjecting the AWC coating to a thermal treatment at 800 °C for 1 h, only few crystalline phases of oxyapatite crystals were detected with XRD. The thermally treated AWC at 800 °C was bioactive, since a bone-like apatite was visible after the first week in SBF. The bioactivity behaviour of the thermally treated AWC coatings at 800 °C could be attributed to the larger amount of the glassy matrix with respect to the thermally treated AWC coatings at 900 °C.

Overall, the results of the present bioactivity study demonstrated that the as-sprayed AWC and AWP coatings were bioactive materials and the bioactive mechanism of these as-sprayed coatings was similar to that of bioactive glasses as proposed by Hench. Moreover, the bioactivity of the AWC and AWP glass–ceramic coatings depended mainly on the amount of the glassy matrix and the amount of Al_2O_3 in the composition.

The prospects for utilisation of the AWC and AWP coatings on titanium alloy implants, especially for load bearing applications, are promising.

Acknowledgments

The authors would like to thank Prof. C. Siligardi (University of Modena and Reggio Emilia). Ravi Kumar (Indian Institute of Technology, Kanpur) is acknowledged for the collaboration in performing the thermal treatments on AWC and Sandro Pizzolante for the in vitro tests. Thanks also to Dr. Maria Cannio for her help with the ICP-AES testing. This work was partially supported by MIUR (Funds "Programmi per l'incentivazione del processo di internazionalizzazione del sistema universitario"). Prof. Sampath acknowledges partial support from the National Science Foundation for this work under award CMMI-0605704. AWC frits were supplied by Colorobbia (Italy).

References

1. Cao, W. and Hench, L. L., Bioactive materials. *Ceramics International*, 1996, **22**, 493–507.
2. Hench, L. L., Bioceramics, a clinical success. *American Ceramic Society Bulletin*, 1998, **7**, VII.
3. Hench, L. L., Bioceramics. *Journal of American Ceramic Society*, 1998, **81**, 1705–1728.
4. Hench, L. L., Bioceramics: from concept to clinic. *Journal of American Ceramic Society*, 1991, **74**, 1487–1510.
5. De AZa, P. N., De Aza, A. H., Pena, P. and De Aza, S., Bioactive glass and glass–ceramics, Ceramica y Vidro. *Bolletin Sociedad Espanola Ceramica*, 2007, **46**(2), 45–55.
6. Kokubo, T., Ito, S., Huang, T., Hayashi, T., Sakka, S. and Kitsugi, T., CaP-rich layer formed on high-strength bioactive glass–ceramic A–W. *Journal of Biomedical Materials Research*, 1990, **24**, 331–343.
7. Ratner, B. D., Hoffman, A. S., Schoen, F. J. and Lemons, J. E., Biomaterials Science. *An Introduction to Materials in Medicine*. Elsevier Academic Press, 2004.
8. Kokubo, T., Ito, S., Sakka, S. and Yamamuro, T., Formation of a high strength bioactive glass–ceramic in the system MgO–CaO–SiO_2–P_2O_5. *Journal of Materials Science*, 1986, **21**, 536–540.
9. Kokubo, T., Bioactive glass ceramics: properties and applications. *Biomaterials*, 1991, **12**, 155–163.

10. Nakamura, T., Yamamuro, T., Higashi, S., Kokubo, T. and Ito, S., A new glass–ceramic for bone replacement: evaluation of its bonding to bone tissue. *Journal of Biomedical Materials Research*, 1985, **19**, 685–698.
11. Kitsugi, T., Yamamuro, T. and Kokubo, T., Bonding behaviour of a glass–ceramic containing apatite and wollastonite in segmental replacement of the rabbit tibia under load-bearing conditions. *The Journal of Bone and Joint Surgery*, 1989, **71**(2), 264–272.
12. Yoshi, S., Kakutani, Y., Yamamuro, T., Nakamura, T., Kitsugi, T., Oka, M., Kokubo, T. and Takagi, M., Strength of bonding between A–W glass–ceramic and surface of bone cortex. *Journal of Biomedical Materials Research*, 1988, **22**, 327–338.
13. Kitsugi, T., Yamamuro, T., Nakamura, T. and Kokubo, T., The bonding of glass ceramics to bone. *International Orthopaedics*, 1989, **13**, 199–206.
14. Kokubo, T., Kushitani, H., Sakka, S., Kitsugi, T. and Yamamuro, T., Solutions able to reproduce in vivo surface-structure changes in bioactive glass–ceramic A–W. *Journal of Biomedical Materials Research*, 1990, **24**, 721–734.
15. Kokubo, T. and Takadama, H., How useful is SBF in predicting in vivo bone bioactivity? *Biomaterials*, 2006, **27**, 2907–2915.
16. Ohtsuki, C., Kokubo, T. and Yamamuro, T., Compositional dependence of bioactivity of glasses in the system $CaO–SiO_2–Al_2O_3$: its in vitro evaluation. *Journal of Materials Science: Materials in Medicine*, 1992, **3**, 119–125.
17. Juhasz, J. A., Best, S. M., Bonfield, W., Kawashita, M., Miyata, N., Kokubo, T. and Nakamura, T., Apatite-forming ability of glass–ceramic apatite–wollastonite–polyethylene composites: effect of the filler content. *Journal of Materials Science: Materials in Medicine*, 2003, **14**, 489–495.
18. Park, J. and Ozturk, A., Tribological properties of $MgO–CaO–SiO_2–P_2O_5$–F-based glass–ceramic for dental applications. *Materials Letters*, 2006, **61**, 1916–1921.
19. Kamitakara, M., Ohtsuki, C., Inada, H., Tanihara, M. and Miyazaki, T., Effect of ZnO addition on bioactive $CaO–SiO_2–P_2O_5–CaF_2$ glass–ceramics containing apatite and wollastonite. *Acta Biomaterialia*, 2006, **2**, 467–471.
20. Rack, H. J. and Qazi, J. I., Titanium alloys for biomedical applications. *Materials Science and Engineering C*, 2006, **26**, 1269–1277.
21. Sun, L., Berndt, C. C., Gross, K. A. and Kucuk, A., Material fundamentals and clinical performance of plasma-sprayed hydroxyapatite coatings: a review. *Journal of Biomedical Materials Research*, 2001, **58**, 570–592.
22. Zhao, Y., Chen, C. and Wang, D., The current techniques for preparing bioglass coatings. *Surface Review and Letters*, 2005, **12**(4), 505–513.
23. Kweh, S. W. K., Khor, K. A. and Cheang, P., Plasma-sprayed hydroxyapatite (HA) coatings with flame-spheroidized feedstock: microstructure and mechanical properties. *Biomaterials*, 2000, **21**, 1223–1234.
24. Guipont, V., Espanol, M., Borit, F., Llorca-Isern, N., Jeadin, M., Khor, K. A. and Cheang, P., High-pressure plasma spraying of hydroxyapatite powders. *Materials Science and Engineering A*, 2002, **325**, 9–18.
25. Espanol, M., Guipont, V., Khor, K. A., Jeadin, M. and Llorca-Isern, N., Effect of heat treatment on high pressure plasma sprayed hydroxyapatite coatings. *Surface Engineering*, 2002, **18**(3), 213–218.
26. Deram, V., Minichiello, C., Vannier, R. N., Le Maguer, A., Pawlowski, L. and Murano, D., Microstructural characterizations of plasma sprayed hydroxyapatite coatings. *Surface and Coatings Technology*, 2003, **166**, 153–159.
27. Dyshlovenko, S., Pateyron, B., Pawlowski, L. and Murano, D., Numerical simulation of hydroxyapatite powder behaviour in plasma jet. *Surface and Coatings Technology*, 2004, **179**, 110–117.
28. Lu, Y., Xiao, G., Li, S., Sun, R. and Li, M., Microstructural inhomogeneity in plasma-sprayed hydroxyapatite coatings and effect of post-heat treatment. *Applied Surface Science*, 2006, **252**(6), 2412–2421.
29. Schrooten, J. and Helsen, J. A., Adhesion of bioactive glass coating to Ti–6Al–4V oral implant. *Biomaterials*, 2000, **2**, 1461–1469.
30. Goller, G., The effect of bond coat on mechanical properties of plasma sprayed Bioglass-titanium coatings. *Ceramics International*, 2004, **30**, 351–355.
31. Vernè, E., Ferraris, M., Jana, C. and Baracchini, L., Bioverit® I base glass/Ti particulate biocomposite: "in situ" vacuum plasma spray deposition. *Journal of the European Ceramic Society*, 2000, **20**, 473–479.
32. Chern Lin, J. H., Lin, H. J., Ding, S. J. and Ju, C. P., Characterization of immersed hydroxyapatite–bioactive glass coatings in Hank's solution. *Materials Chemistry and Physics*, 2000, **64**, 229–240.
33. Carvalho, F. L. S., Borges, C. S., Branco, J. R. T. and Pereira, M. M., Structural analysis of hydroxyapatite/bioactive glass composite coatings obtained by plasma spray processing. *Journal of Non-Crystalline Solids*, 1999, **247**, 64–68.
34. Lee, T. M., Chang, E., Wang, B. C. and Yang, C. Y., Characteristics of plasma-sprayed bioactive glass coatings on Ti–6A1–4V alloy: an in vitro study. *Surface and Coatings Technology*, 1996, **79**, 170–177.
35. Gabbi, C., Cacchioli, A., Locardi, B. and Guadagninol, E., Bioactive glass coating: physicochemical aspects and biological findings. *Biomaterials*, 1995, **16**, 515–520.
36. Silva, P. L., Santos, J. D., Monteiro, F. J. and Knowles, J. C., Adhesion and microstructural characterization of plasma-sprayed hydroxyapatite/glass ceramic coatings onto Ti–6A1–4V substrates. *Surface and Coatings Technology*, 1998, **102**, 191–196.
37. Chang, C. K., Mao, D. L. and Wu, J. S., Characteristics of crystals precipitated in sintered apatite/wollastonite glass ceramics. *Ceramics International*, 2000, **26**, 779–785.
38. Bolelli, G., Cannillo, V., Lusvarghi, L. and Manfredini, T., Glass alumina composite coatings by plasma spraying. Part I. Microstructural and mechanical characterization. *Surface and Coatings Technology*, 2006, **201**, 458–473.
39. Bolelli, G., Lusvarghi, L., Manfredini, T. and Siligardi, C., Influence of the manufacturing process on the crystallization behaviour of a CZS glass system. *Journal of Non-Crystalline Solids*, 2005, **351**, 2537–2546.
40. Helsen, J. A. *et al.*, Glasses and bioglasses: synthesis and coatings. *Journal of the European Ceramic Society*, 1997, **17**, 147–152.
41. Peitl, O., Zanotto, E. D. and Hench, L., Highly bioactive $P_2O_5–Na_2O–CaO–SiO_2$ glass–ceramics. *Journal of Non-Crystalline Solids*, 2001, **292**, 115–126.
42. Liu, D., Bioactive glass–ceramic: formation, characterisation and bioactivity. *Materials Chemistry and Physics*, 1994, **36**, 294–303.
43. Salama, S. N., Darwish, H. and Abo-Mosallam, H. A., HA forming ability of some glass–ceramics of the $CaMgSi_2O_6–Ca_5(PO_4)_3F–CaAl_2SiO_6$ system. *Ceramics International*, 2006, **32**, 357–364.
44. Andersson, O. H. and Sodergard, A., Solubility and film formation of phosphate and alumina containing silicate glasses. *Journal of Non-Crystalline Solids*, 1999, **246**, 9–15.
45. Lee, Y., Wang, C., Huang, T., Chen, C., Kao, C. and Ding, S., In vitro characterisation of post heat-treated plasma-sprayed hydroxyapatite coatings. *Surface & Coatings Technology*, 2005, **197**, 367–374.
46. Karlsson, K. H., Froberg, K. and Ringbom, T., A structural approach to bone adhering of bioactive glasses. *Journal of Non-Crystalline Solids*, 1989, **112**, 69–72.